Experimental study on the dynamic mechanical response of a blue light-stimulated acrylate side chain liquid crystal elastomer

Li, Zichuan; Wymenga, Luutzen; Fan, Jiajie; Zhang, Guoqi

DOI
10.1364/OL.533577

Publication date
2024

Document Version
Final published version

Published in
Optics Letters

Optics Letters

Experimental study on the dynamic mechanical response of a blue light-stimulated acrylate side chain liquid crystal elastomer

ZICHUAN LI,[1] LUUTZEN WYMENGA,[1] JIAJIE FAN,[1,2] AND GUOQI ZHANG[1,*]

[1] Faculty Electrical Engineering, Mathematics and Computer Science, Delft University of Technology, Delft, 2628 CD, The Netherlands
[2] Academy for Engineering & Technology, Shanghai Engineering Technology Research Center for SiC Power Device, Fudan University, Shanghai 200433, China
*G.Q.Zhang@tudelft.nl

Received 26 June 2024; revised 19 August 2024; accepted 20 August 2024; posted 23 August 2024; published 11 September 2024

This study demonstrates a breakdown analysis of the dynamics of a liquid crystal elastomer (LCE) including quality check, geometric measurement, thermal characterization, and comparison of heat- and light-induced contractions. A blue light-responsive acrylate side chain LCE with 1% azobenzene dye was characterized. From a classical viewpoint, photo-thermal contraction is considered a dominating effect, while direct photo-mechanical deformation can be neglected due to a low dye percentage. However, the findings of this research suggest that a low percentage of azobenzene dye does not necessarily lead to heat-dominating dynamics of LCE. This phenomenon has not yet been quantitatively studied before. The approach reported in this Letter can potentially be used to extract the data to improve the dynamics models of light-driven LCEs.

https://doi.org/10.1364/OL.533577

Introduction. Combining the elasticity of elastomers with the multiphysics sensitivity of liquid crystals, liquid crystal elastomers (LCEs) are considered promising materials for soft robotic actuators. LCEs could be actuated by light through the incorporation of doped azobenzene dye molecules [1]. Light-driven LCEs as remotely controllable soft robots have been widely explored, for instance, self-regulating iris [2], light-driven motor [3], photo-thermal oscillators [4], gripper [5], microfluidic chip [6], and continuously tunable intensity modulators [7]. Possibly, LCEs could be used to restore the mechanical functions of organs since the mechanical properties of LCEs are generally similar to natural muscles [8]. A recently developed azobenzene-dyed side chain acrylate LCE is a promising candidate for an LCE-based cardiac assist device [9]. Its unique advantages for biomedical applications include low glass transition temperature T_g of around 25°C, sub-second actuation, visible light sensitivity, and cell compatibility [10].

As the blue light emitting diode (LED) has very high energy efficiency, the LCE was made blue light-responsive by a chemically modified azobenzene dye. The dynamic behaviors of the optimized LCE have been reported in the literature [11]. However, the methodology has two major drawbacks: i) The tests were conducted at room temperature that is lower than T_g. This may overestimate the mechanical output of the LCE at a continuous working condition with an average temperature above T_g; ii) The local temperature of LCE samples was not measured or calculated. This could lead to wrongful prediction of dynamic behaviors of LCE in different heat dissipation conditions. A systematical characterization routine needs to be established to put the LCE actuator further toward practical application. The theoretical modeling for the dynamic behaviors of light-driven LCE is far from mature though the liquid crystals [12] and polymers themselves have been studied in deep. The photoinduced heating and direct photo-mechanical effects of azobenzene dyes can both power the spontaneous deformation of LCE. However, their individual contributions to the mechanical output are not always properly captured by the widely used classical model proposed by [1].

This Letter demonstrates an experimental workflow to systematically and rapidly characterize a light-driven LCE. The method consists of a quick assessment of the quality of LCE samples, contactless temperature tracking of LCE under illumination, and passive and active mechanical properties of LCE. First, we use polarized light and indirect mechanical measurement to check the uniformity and thickness of synthesized LCE samples. The uniaxial tension test was used to determine the passive modulus along the nematic director of the LCE. The infrared (IR) camera was used to observe the relation between the temperature of the sample in air and light intensity. Both pure heat-induced and light-driven mechanical responses were quantified using temperature-controlled Dynamical Mechanical Analysis (DMA). The proposed approach can potentially be used to extract the key parameters for a fully coupled multiphysics model of LCE.

Experiment. A blue light-responsive side chain end-on LCE with an acrylate polymeric backbone was created as described in [13,14]. Figure 1 shows the mixture of monomers. The acrylate network crosslinked by RM257 provides the LCE with a reversible shape change. The percentage of crosslinkers has a significant impact on the mechanical properties of LCE and, therefore, has been optimized in previous studies [9,11]. Rod-like mesogenic moieties C6BP tend toward ordered alignment,

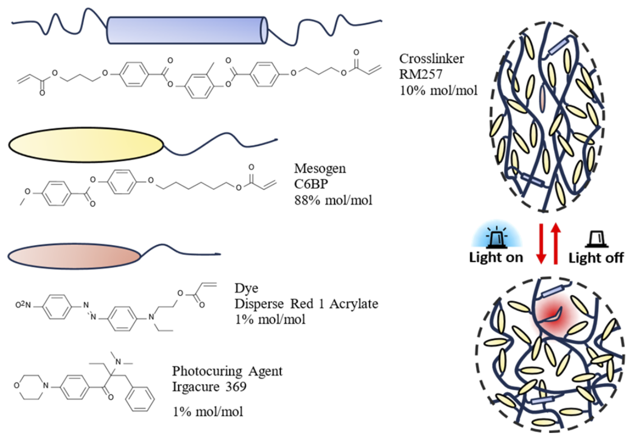

Fig. 1. Composition of blue light-responsive side chain end-on acrylate LCE.

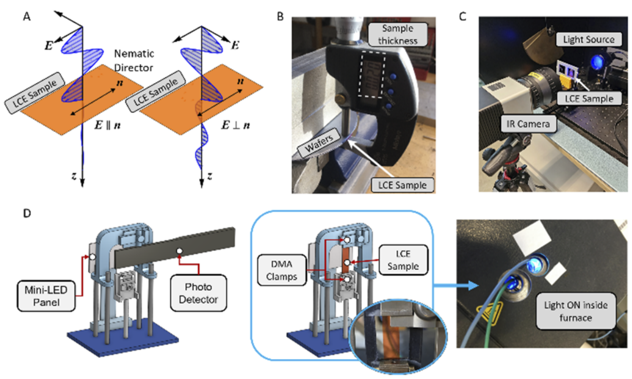

Fig. 2. (A) Quality check with polarized light; (B) subtractive thickness measurement; (C) measurement of thermal parameters; (D) DMA test of the mechanical response of LCE. The mini-LED array provides controllable homogeneous illumination to the LCE strips. The built-in furnace of the DMA machine controls the temperature and blocks the environmental light.

which leads to an anisotropic polymeric coil shape. Irgacure 369 is the photocuring agent that promotes polymerization. The azobenzene dye Disperse Red 1 (DR1) acrylate embedded in the LCE network is the source of the light sensitivity of LCE. External stimuli can change the shape of polymeric coils in LCE and cause spontaneous deformation. In the classical theory, light-induced heating is a dominating mechanism for the current LCE since the concentration of azo-dye is as low as 1% [15]. In this research, we conducted the breakdown analysis below to falsify this theory.

The anisotropic optical properties of LCE provide us with an efficient approach to checking the uniformity of the LCE film (Fig. 2(A)). The mesogenic dye molecule tends to absorb the light polarized along the direction **E** that is parallel to its direction [16,17]. The evenness of transmittance of the samples indicates the uniformity of the LCE film. The thickness of each LCE film was subtractively measured multiple times ($n \geq 5$) by gently placing the sample between two silicon wafers with thickness of 0.5 mm, using a micrometer (Mitutoyo IP65, USA) (Fig. 2(B)).

An infrared (IR) camera (*Infratec VarioCam 800HD*) equipped with a close-up lens of 0.5× to 60 mm was used to observe the heat transfer parameters of the LCE samples (Fig. 2(C)). A blue (470 nm) light source (Thorlabs M470L3) with a collimating lens (ThorLabs COP1-A) provided far-field illumination. The LCE sample was placed at the focus of the light source. The local light intensity measured with a photometer (Thorlabs PM400) was 1.7 mW/mm^2. Equation (1) is the governing equation of the LCE temperature T under illumination obtained via a lumped system analysis (see Supplement 1 for supporting content):

$$T(t) \approx \begin{cases} T_{air} + \Delta T_{\max}[1 - \exp(-t/\tau_{HT})] & \text{for actuation} \\ T_{air} + \Delta T_{\max}\exp(-t/\tau_{HT}) & \text{for relaxation} \end{cases}, \quad \textbf{(1)}$$

where t is the elapsed time from the start of an actuation or relaxation stage; $\Delta T_{\max} = I/2k_{air}$ denotes the maximum temperature increase that an illumination I can cause with a surface heat transfer coefficient k_{air}; $\tau_{HT} = C_p h/2k_{air}$ denotes the characteristic time of light-induced heating in an LCE with a thickness of h, which is 2.8 s for a 20 μm sample; C_p is the heat capacity. Deducing from the temperature curve in IR results (see Supplement 1 for supporting content), the heat capacity C_p is 1.918 J/(K·cm^3), and the surface heat transfer coefficient of LCE to air k_{air} is 1.37 mW/(K·cm^2). Both values are in a reasonable range for acrylate polymers.

Figure 2(D) shows the procedure for measuring the photoinduced mechanical response of LCE samples. The test was conducted in the DMA machine with a furnace (*TA Instruments DMA Q800*). A customized blue light mini-LED panel provided controllable illumination inside the furnace to power the contraction of the LCE. The homogeneity of the irradiance pattern of the mini-LED panel was well-optimized in the design stage. The relationship between the input current and local light intensity on the sample's position was calibrated using the photometer mentioned above. The LCE films were cut into thinner strips with a size of about 5 × 20 mm^2. Two ends of LCE strips were glued to paper frames to protect the samples from local failure on the clamped regions.

Results and discussion. The storage modulus E of LCE was first tested via a uniaxial tension test on the DMA machine. In general, the LCE material has complicated three-dimensional anisotropic mechanical properties. However, we focus only on the spontaneous contraction along the nematic director in this research and use a uniaxial model to model the behavior. The tension rate was set to be low to exclude the impact of viscosity on the results. Figure 3 shows the stress–strain curves obtained from the passive tensile test at 37°C using seven samples with thicknesses of 20–28 μm (Table S1). A consistency in slopes is found among all tested LCE samples. Meanwhile, the tensile strengths vary from sample to sample. This can be attributed to the stochastic holes and imperfections generated during the synthesis of LCE films. As a reference, two thicker LCE strips with about 55 μm in thickness were also tested to evaluate the potential size effect in passive mechanical properties. The evaluated moduli of thicker LCE strips have no significant difference from the ones of 20 μm samples, suggesting that the size-dependent effect in passive mechanical properties can be neglected. One of the thick samples showed a significantly high tensile strength. Thicker samples may have a lower possibility of having penetrating voids, which may significantly lower the strength of the LCE material. The average modulus E over samples within the strain range of 0.1–4% is 11 MPa with a standard deviation (SD) of 0.81 Mpa.

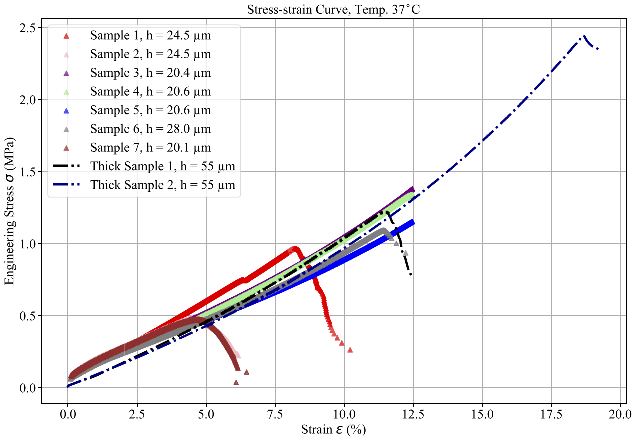

Fig. 3. Passive tensile test on LCE samples. Two samples with a thickness of 55 μm were used as a reference. The unevenness and random small holes in the material may affect the breaking strength.

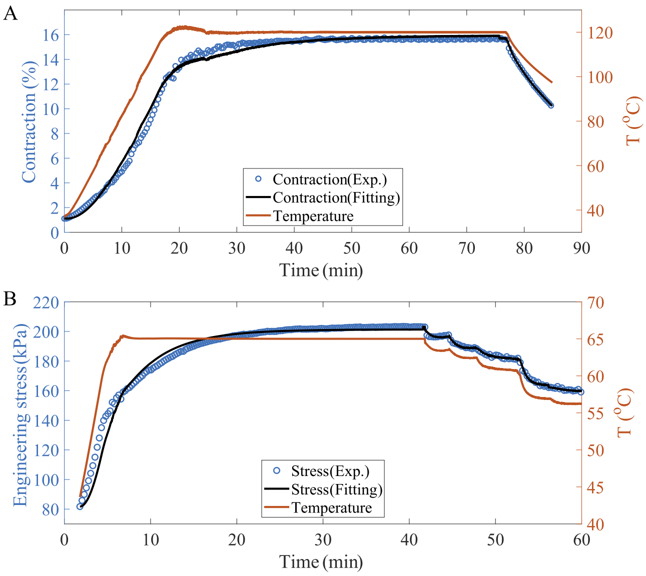

Fig. 4. Heat actuation of LCE in a dark environment. (A) Thermal contraction. The pre-load was set to be 0.1 mN to make the boundaries of LCE approximately free; (B) actuation stress of LCE with both ends fixed.

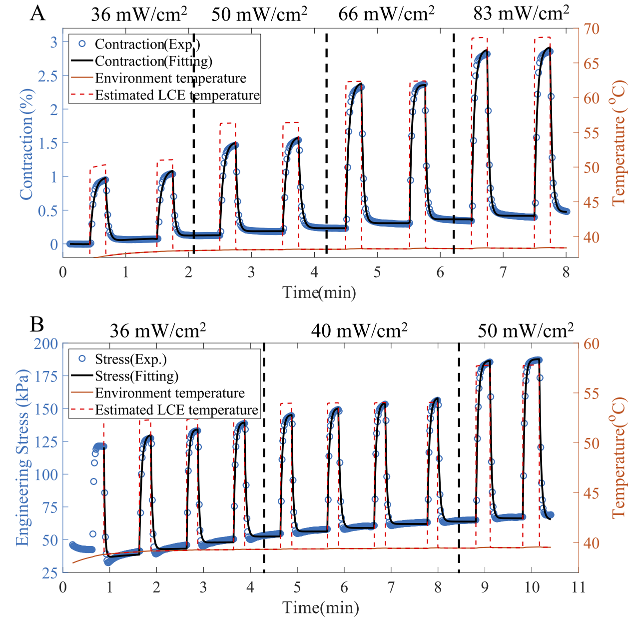

Fig. 5. Light-driven contraction of LCE and temperature. (A) LCE free contraction. The pre-load was set to be 0.1 mN to make the boundary of LCE approximately free; (B) stress produced by LCE with both sides fixed.

Figure 4 shows the pure heating-induced responses of the LCE strips at two boundary constraints, i.e., free contraction and fixed-ends. The start points of both curves are not zero since samples were installed at room temperature while the data was collected after a 10 min relaxation at a temperature of 37°C ($>T_g$). We consider an exponential evolution of the mechanical response to the change in temperature

$$M(t) = M_0 + \alpha_M (T - T_0) \left[1 - \exp\left(-\frac{t}{\tau_M} \frac{T_0}{T} \right) \right], \qquad (2)$$

where M represents the contraction ε for the free contraction test and engineering stress σ for the fixed-end test; α_M is the coefficient of the mechanical response M; τ_M is the time constant of M. The lower indices 0 refer to the values of quantities at the initial time. The fittings in Figs. 4 and 5 are done via a piecewise approach. The time domain is split into actuation stage(s) and relaxation stage(s) (see Supplement 1 for supporting content).

A significant delay in the mechanical response to temperature increases can be observed in both cases. The black curves in Fig. 4 are drawn with the fitted parameters α_M and τ_M. At the heating stage of the free deformation case, the fitted α_ε and τ_ε are 0.179%/K and 12 min, respectively. However, the characteristic time τ_ε is at a level of <1 s at the cooling stage. At the heating stage of the fixed-end case, fitted α_σ and τ_σ are 5.60 kPa/K and 4.66 min, respectively. At the cooling stage, the characteristic time τ_σ reduces to a quarter of the value at the heating stage, i.e. about 1.18 min. Compared to the free condition, the LCE has a lower characteristic time, meaning the external pre-loading can promote the actuation of the LCE. In both boundary conditions, the LCE shows a rapid relaxation when cooling. Substituting the modulus measured in the passive tension test to Eq. (2), the theoretical actuation stress at the fixed-end condition can be calculated via $\sigma_T = \alpha_\varepsilon E \Delta T$, and its result is 394 kPa at a temperature increase of 20 K. In contrast, Fig. 4(B) shows a much lower maximum actuation stress of 120 kPa. This can be attributed to the heat-induced softening of LCE.

The photo-actuation of LCE strips at two different boundary conditions is shown in Fig. 5. The duration of each light pulse is set to 15 s. This duration can achieve a stationary temperature for the characteristic light-induced heating is only 2.8 s according to the IR measurement. The local temperature in the LCE strip is calculated via Eq. (1) since the *in situ* temperature of the sample is hard to measure. Substituting the temperature calculated by Eq. (1) into Eq. (2) leads to a function for the light actuation of LCE strips.

The estimated temperature increases caused by the four light intensities (36, 50, 66, and 83 mW/cm^2) in the free contraction test are about 10.6, 14.7, 19.4, and 24.4 K, respectively. The change in environment temperature is much smaller than the one in the sample temperature, indicating that the heat generated in the LED panel makes an acceptable impact on the measurement. The fitted α_ε and τ_ε are 0.077%/K (SD = 0.067%/K) and 2.5 s (SD = 0.56 s), respectively. In the fixed-end test, light with three intensities of 36, 40, and 50 mW/cm^2 are applied to the LCE strip. The corresponding temperature increases are about 10.6, 11.8, and 14.7 K, respectively. The fitted α_σ and τ_σ are 6.4 kPa/K (SD = 0.22 kPa/K) and 2.3 s (SD = 0.22 s), respectively. The linear coefficients α_ε and α_σ control the maximum mechanical responses that the LCE can achieve by an increase in local temperature. Compared to the values obtained in the pure heat-driven test, the light stimuli can cause a 40–60% weaker spontaneous contraction with the same temperature increase. However, the stress produced by light is 15–20% higher. The light-induced mechanical responses are significantly more rapid than the heat-induced ones. Besides, the difference in the time constant of the actuation stages and the relaxation stages is negligible in the light-driven tests. The total different dynamic characteristics of heat- and light-driven indicate that azobenzene dyes in a low percentage of 1% can still promote the dynamics of light-driven LCE actuators via some photochemical mechanisms. The comparison between free deformation and fixed-end tests shows that the proper pre-loading can also improve the speed and amplitude of mechanical response in both heat- and light-driven cases.

Conclusion. This Letter demonstrates a universal experimental workflow to systematically but quickly characterize the dynamics behaviors of a light-driven LCE material. A blue light-responsive side chain end-on acrylate LCE was studied as a case. The complicated photo-thermal actuation of this LCE was studied in a series of breakdown experiments. In the end, the LED-driven contraction of LCE was measured on the DMA platform to examine the concept. The results show good self-consistency and quantitatively demonstrate that a low percentage of azobenzene dye (e.g. 1% in this study) does not necessarily lead to negligible direct photo-mechanical or heat-dominating phase transition dynamics of LCE. Therefore, the interpretation of how isomerization affects light actuation of LCE is not a complete story yet despite massive models proposed over the last two decades. The reported approach can potentially be used to extract the key parameters for a fully coupled multiphysics dynamics model of LCE.

Funding. European Union Horizon 2020 Framework Programme research and innovation program (952166).

Acknowledgment. The authors thank Camilla Parmeggiani and Daniele Martella from the European Laboratory for Non-Linear Spectroscopy (LENS) for the sample preparation, Kasper Jansen from the Faculty of Industrial Design Engineering (IDE) of Delft University of Technology for the training in DMA setup, Remko Seijffers from the faculty of Mechanical, Maritime and Material (3mE) of Delft University of Technology for the support in IR test. European Union Horizon 2020 research and innovation program under grant agreement No. 952166.

Disclosures. The authors declare no conflicts of interest.

Data availability. Data underlying the results presented in this paper are not publicly available at this time but may be obtained from the authors upon reasonable request.

Supplemental document. See Supplement 1 for supporting content.

REFERENCES

1. H. Finkelmann, E. Nishikawa, G. G. Pereira, *et al.*, Phys. Rev. Lett. **87**, 015501 (2001).
2. H. Zeng, O. M. Wani, P. Wasylczyk, *et al.*, Adv. Mater. **29**, 1701814 (2017).
3. M. Yamada, M. Kondo, J. Mamiya, *et al.*, Angew. Chem. Int. Ed. **47**, 4986 (2008).
4. A. H. Gelebart, G. Vantomme, E. W. Meijer, *et al.*, Adv. Mater. **29**, 1606712 (2017).
5. A. W. Long and A. L. Ferguson, Mol. Syst. Des. Eng. **3**, 49 (2018).
6. Y. Lu, L. Qin, Q. Liu, *et al.*, NPG Asia Mater. **14**, 73 (2022).
7. W.-F. Chiang, H. M. Silalahi, Y.-C. Chiang, *et al.*, Opt. Express **28**, 27676 (2020).
8. M. Ilami, H. Bagheri, R. Ahmed, *et al.*, Adv. Mater. **33**, e2003139 (2021).
9. C. Ferrantini, J. M. Pioner, D. Martella, *et al.*, Circ. Res. **124**, e44 (2019).
10. D. Martella, P. Paoli, J. M. Pioner, *et al.*, Small **13**, 1702677 (2017).
11. G. Vitale, B. Grandinetti, S. Querceto, *et al.*, Macromol. Mater. Eng. **307**, 2200187 (2022).
12. A. M. Sonnet and E. G. Virga, *Dissipative Ordered Fluids: Theories for Liquid Crystals* (Springer Science & Business Media, 2012).
13. D. Martella, D. Antonioli, S. Nocentini, *et al.*, RSC Adv. **7**, 19940 (2017).
14. H. Zeng, D. Martella, P. Wasylczyk, *et al.*, Adv. Mater. **26**, 2319 (2014).
15. D. Martella, S. Nocentini, F. Micheletti, *et al.*, Soft Matter **15**, 1312 (2019).
16. C. L. Harvey and E. M. Terentjev, Eur. Phys. J. E. **23**, 185 (2007).
17. D. Corbett and M. Warner, Phys. Rev. E **78**, 061701 (2008).